Automatica 149 (2023) 110811

Contents lists available at ScienceDirect

Automatica

journal homepage: www.elsevier.com/locate/automatica

Brief paper

Justification of the geometric solution of a target defense game with faster defenders and a convex target area using the HJI equation ☆

Han Fu *, Hugh H.-T. Liu

University of Toronto, 4925 Dufferin Street, North York, M3H 5T6, Ontario, Canada

ARTICLE INFO

Article history:
Received 26 September 2021
Received in revised form 22 September 2022
Accepted 18 November 2022
Available online 3 January 2023

Keywords:
Target defense
Differential game
HJI equation
Viscosity solution

ABSTRACT

A multi-defender single-invader target defense game is a differential game where the invader intends to enter a target area protected by a group of defenders, while the defenders intend to capture the invader before it enters. This game has been extensively studied and a geometric solution exists. However, this solution has only been justified under special cases. The main contribution of this paper is to prove that the geometric solution satisfies the HJI equation under the general condition. Specifically, the target area is not required to take a peculiar shape, such as circles, lines, etc. In addition, the defenders are allowed to move freely in the two-dimensional plane, the capture range of the defenders is non-zero, and the number of defenders is not restricted. This generalized formulation imposes an important challenge on an essential step of the proof, computing the derivatives of the value function. This challenge is resolved in this paper therefore the proof can be accomplished. The significance of studying the geometric solution is that it provides a state feedback control law using an adequate amount of computation. The target defense game is inherently challenging to be solved with numerical methods, because it is highly nonlinear and suffers from the curse of dimensionality. The proof presented in this paper provides a solid theoretic foundation for the geometric solution, so the difficulties raised by the numerical methods can be circumvented.

1. Introduction

The target defense differential game is a mathematical abstraction of the counter-UAV scenario where a specific area needs to be protected against hostile drones (Michel & Holland, 2018; Sathyamoorthy, 2015). The differential game theory was initialized by Isaacs in his seminal book (Isaacs, 1999), where the Hamilton–Jacobi–Bellman–Isaacs (HJI) equation was constructed and a solution was proposed using dynamic programming. Such method was used to obtain analytical solutions for a number of games (Hagedorn & Breakwell, 1976; Merz, 1971, 1972). As a partial differential equation (PDE), the HJI equation can be solved numerically. For example, it can be converted into a fixed-point problem (Falcone, 2006), or can be treated as the function of a time-varying curve (Fisac, Chen, Tomlin, & Sastry, 2015; Margellos & Lygeros, 2011) and solved with the level-set method (Mitchell, 2007; Mitchell, Bayen, & Tomlin, 2005). The game can also be split as coupled optimization problems and solved as a nonlinear programming (Carr, Cobb, Pachter, & Pierce, 2018). However, numerical solutions suffer from curse of dimensionality, the fact that the computation cost increases exponentially with the problem dimension. Adaptive dynamic programming (ADP) (Rubies-Royo & Tomlin, 2016; Vamvoudakis & Lewis, 2011) and reinforcement learning (RL) (Dixon, 2014; Lowe et al., 2017) are powerful in addressing these problems, but the target defense game is still tricky because its objective function does not contain an integral term.

Due to the reasons above, analytical solutions remain a popular option in the study of differential games. To facilitate the analytical solution, the formulation of the game is important. For example, players are usually modeled as single integrators (Fuchs, Khargonekar, & Evers, 2010; Scott & Leonard, 2014) or unicycles (Scott & Leonard, 2018). Choosing proper state variables (Wei & Yang, 2018) and decomposing complex games into subproblems (Shishika & Kumar, 2018; Zha, Chen, Peng, & Gu, 2016) are commonly used techniques. Meanwhile, intuitions and geometric methods also play an important role, among which an extensively studied concept is the dominance region (Isaacs, 1999), the area that one player can reach before all the other players. When the defender's capture range is zero, the invader's dominance region in a single defender game is an Apollonius circle (Dorothy, Maity, Shishika, & Von Moll, 2021; Ramana & Kothari, 2017; Wang, Yue, & Liu, 2015; Yan, Shi, & Zhong, 2021).

☆ The material in this paper was not presented at any conference. This paper was recommended for publication in revised form by Associate Editor Andrey V. Savkin under the direction of Editor Ian R. Petersen.
* Corresponding author.
E-mail addresses: flora.fu@mail.utoronto.ca (H. Fu), hugh.liu@utoronto.ca (H.H.-T. Liu).

https://doi.org/10.1016/j.automatica.2022.110811
0005-1098/

When the capture range is non-zero, the dominance region becomes a Cartesian oval (Garcia & Bopardikar, 2021). A limitation of the intuitive solution is the lack of strict justification. An example is the game of capturing two evaders. A natural intuition is the pursuer capturing the evaders subsequently. Unfortunately, the game has a stage where the pursuer has equal distances from both evaders (Breakwell & Hagedorn, 1979), and the game only degrades into a single-evader game when the pursuer breaks the tie by selecting one evader. Another example is the multi-pursuer single-evader game, where the intuitive control law (Von Moll, Casbeer, Garcia, Milutinović, & Pachter, 2019) was found to be optimal in only part of the state space (Pachter, Moll, Garcia, Casbeer, & Milutinović, 2020).

Differential games have rich variations. Aside from the most popularly studied pursuit-evasion game, Ref. Garcia, Casbeer, Tran, and Pachter (2021) solved a multiplayer game where the players are able to attack opponents within a given range, Ref. Szőts and Harmati (2019) proposed a method for slower pursuers to capture a faster evader. Weintraub, Von Moll, Garcia, Casbeer, and Pachter (2022) designed a strategy to track a moving target with a slower observer agent. A recent study (Szőts, Savkin, & Harmati, 2021) presented an alternative solution for the problem studied in Hagedorn and Breakwell (1976) to handle singularities. A perimeter defense game where the defenders moved along the boundary of the target area was solved in Shishika and Kumar (2019, 2020), Von Moll, Pachter, Shishika, and Fuchs (2020), and its variations with multiple players (Shishika, Paulos, & Kumar, 2020) and in three-dimensional spaces (Lee, Shishika, & Kumar, 2020) were also investigated. A similar perimeter defense game was studied where the invaders intended to leave the target area from inside (Marzoughi & Savkin, 2021). In Yan, Shi, and Zhong (2018, 2019), an analytical solution was proposed for guarding a linear target area within a rectangular region. The solution made extensive use of the dominance region.

This paper studies a target defense game where the defenders move freely in an unbounded two-dimensional plane. Although this game has a geometric solution (Isaacs, 1999) and has been extensively studied (Fu & Liu, 2020; Garcia, Casbeer, & Pachter, 2020), it has only been proved for special cases to the authors' best knowledge. For example, when the target area is linear (Garcia, Von Moll, Casbeer, & Pachter, 2019), circular and polygonal (Pachter, Garcia, & Casbeer, 2017). The work in Lee and Bakolas (2021) provided a justification for convex target areas, but the game involved only one defender. In addition, proofs in Garcia et al. (2019), Lee and Bakolas (2021) and Pachter et al. (2017) all assumed zero capture range.

The contribution of this paper is a justification of the geometric using the HJI equation. We resolve three challenges. Firstly, validating the geometric solution requires to compute the partial derivatives of the function representing the target area, which is arbitrarily convex thus has no specific expression. Lee and Bakolas (2021) handled this problem by constructing a function that described the distance from a point to the target area. Such construction is not required in this paper. Secondly, the non-zero capture range makes the boundary of the dominance region a fourth order curve, causing the analytical representation of a critical intermediate variable become extremely complex. Such representation was essential in Garcia et al. (2019), Lee and Bakolas (2021) and Pachter et al. (2017) but is not required in this paper. Thirdly, the value function suggested by the geometric solution is not differentiable when multiple defenders are involved. Through a detailed classification of possible situations of the game, we prove the value function to be continuous thus it solves the HJI equation in the viscosity sense (Crandall & Lions, 1983).

The rest of the paper is organized as follows. Section 2 formulates the multi-defender single-invader (MDSI) target defense game and introduces the geometric solution. Section 3 proves the geometric solution for the single-defender single-invader (SDSI) game. Section 4 proves the geometric solution for the MDSI game and presents several simulations. Section 5 concludes the study of this paper and discusses potential future works. An Appendix is attached which includes detailed derivations of the proof.

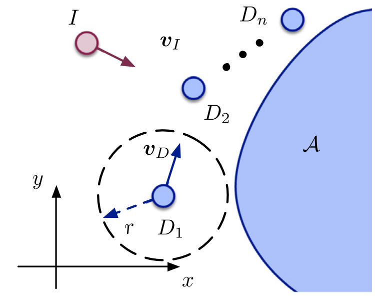

Fig. 1. Definition of the MDSI game.

2. Problem description

2.1. Formulation of the MDSI game

Consider a target area $\mathcal{A}$, a group of defenders $D_j, j = 1, \dots, n$ and a single invader I, as shown in Fig. 1. Assume

A1 the target area $\mathcal{A}$ is convex, and can be represented as

$$\mathcal{A} = \left\{[x, y]^T | \phi(x, y) \le 0\right\}, \tag{2.1}$$

where $\phi(x, y) : \mathbb{R}^2 \to \mathbb{R}$ is second order differentiable.

A2 The players' sizes and turning radii are much smaller than their traveling distances, thus the dynamics of the system can be described as

$$\begin{aligned} &\dot{x}_j = v_{x_j}, \quad \dot{y}_j = v_{y_j}, \quad \sqrt{v_{x_j}^2 + v_{y_j}^2} = v_D, \quad j = 1, \dots, n \\ &\dot{x}_I = v_{x_I}, \quad \dot{y}_I = v_{y_I}, \quad \sqrt{v_{x_I}^2 + v_{y_I}^2} = v_I. \end{aligned} \tag{2.2}$$

where $[x_j, y_j]^T = \boldsymbol{p}_j$, $[x_I, y_I]^T = \boldsymbol{p}_I$ are positions of the jth defender and the invader, $[v_{x_j}, v_{y_j}]^T = \boldsymbol{v}_j$, $[v_{x_I}, v_{y_I}]^T = \boldsymbol{v}_I$ are player velocities and control inputs, v_D, v_I are velocity magnitudes.

A3 The defenders travel faster, i.e., $v_D \ge v_I$, or $a > 1$, where

$$a = v_D/v_I. \tag{2.3}$$

In the game, the invader intends to enter the target area without being captured, while the defenders seek to capture the invader outside of the target. Capture happens when the invader is within the capture range r of at least one defender, i.e., $\exists j \in \{1, \dots, n\}$ s.t. $\|\boldsymbol{p}_I - \boldsymbol{p}_j\| \le r$. Assume

A4 the capture range is positive, i.e., $r > 0$.

Remark 2.1. As will be revealed later, the proposed proof has no requirement on r. Therefore the proof is also valid for $r = 0$.

Let $[x_I^c, y_I^c]^T$ be the invader's location upon capture, the game is defined by Eq. (2.4), where V is the value function.

$$V(x_1, y_1, \dots, x_n, y_n, x_I, y_I) = \min_{\boldsymbol{v}_I} \max_{\boldsymbol{v}_1, \dots, \boldsymbol{v}_n} \phi(x_I^c, y_I^c). \tag{2.4}$$

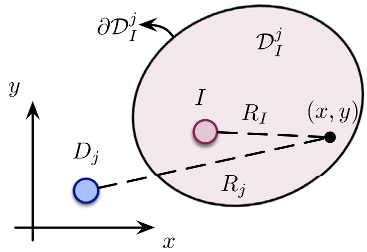

Fig. 2. Dominance region of the invader. Players are massless points therefore D_j, I can also be viewed as positions of defender D_j and invader I.

2.2. Dominance region

The invader's dominance region against a single defender is the area within which any point can be reached by the invader without capture, as shown in Fig. 2 and defined in (2.5).

$$\mathcal{D}_I^j = \left\{[x, y]^T | d^j(x, y, x_j, y_j, x_I, y_I) \geq 0\right\}, \tag{2.5a}$$

$$d^j(x, y, x_j, y_j, x_I, y_I) = R_j(x, y) - aR_I(x, y) - r, \tag{2.5b}$$

$$\begin{aligned} R_j(x, y) &= \sqrt{(x - x_j)^2 + (y - y_j)^2}, \\ R_I(x, y) &= \sqrt{(x - x_I)^2 + (y - y_I)^2}. \end{aligned} \tag{2.5c}$$

When there are multiple defenders, the overall dominance region of the invader is the intersection of all the individual dominance regions. i.e., $\mathcal{D}_I = \cap_{j=1,\dots,n}\mathcal{D}_I^j$.

Lemma 2.1. *For given player locations, dominance region $\mathcal{D}_I = \cap_{j=1,\dots,n}\mathcal{D}_I^j$ is convex.*

Lemma 2.1 is proved in Appendix C.

Since any point within the invader's dominance region can be reached by the invader without capture, if $\mathcal{A}\cap\mathcal{D}_I \neq \emptyset$, the invader wins regardlessly. To eliminate this trivial case, an additional assumption is imposed:

A5 $\mathcal{A} \cap \mathcal{D}_I = \emptyset$ at the beginning of the game.

2.3. Geometric solution

Given player locations, define an auxiliary problem

$$P_{aux}(D_1, \dots, D_n) : \quad \begin{aligned} &\min_{[x,y]^T} \phi(x, y) \\ &s.t.\ [x, y]^T \in \mathcal{D}_I = \cap_{j=1,\dots,n}\mathcal{D}_I^j \end{aligned}, \tag{2.6}$$

where $D_1, \dots, D_n$ are the defenders involved in the game.

Lemma 2.2. *$P_{aux}(D_1, \dots, D_n)$ is convex and has a unique solution $\boldsymbol{p}^* = [x^*, y^*]^T \in \partial\mathcal{D}_I$. $\partial\mathcal{D}_I$ is the boundary of $\mathcal{D}_I$.*

Proof. Lemma 2.2 is obvious due to the convexity of ϕ and $\mathcal{D}_I$, and assumption A5. □

Then the geometric strategy is given by

$$\begin{aligned} \boldsymbol{v}_j^g(x_1, y_1, \dots, x_n, y_n, x_I, y_I) &= \frac{v_D}{R_j(x^*, y^*)}\begin{bmatrix} x^* - x_j \\ y^* - y_j \end{bmatrix}, \ j = 1, \dots, n, \\ \boldsymbol{v}_I^g(x_1, y_1, \dots, x_n, y_n, x_I, y_I) &= \frac{v_I}{R_I(x^*, y^*)}\begin{bmatrix} x^* - x_I \\ y^* - y_I \end{bmatrix}, \end{aligned} \tag{2.7}$$

and the value function is suggested to be

$$V^g(x_1, y_1, \dots, x_n, y_n, x_I, y_I) = g(x^*, y^*). \tag{2.8}$$

2.4. Goal of the paper

The goal of this paper is to prove the following theorem

Theorem 2.1. *For the target defense game with dynamics (2.2), target area (2.1) and assumptions A1–A5, the geometric control law (2.7) and value function (2.8) solve the HJI equation*

$$\min_{\boldsymbol{v}_I}\max_{\boldsymbol{v}_1,\dots,\boldsymbol{v}_n}\left\{\sum_{j=1}^{n}\left(\frac{\partial V}{\partial x_j}\dot{x}_j + \frac{\partial V}{\partial y_j}\dot{y}_j\right) + \frac{\partial V}{\partial x_I}\dot{x}_I + \frac{\partial V}{\partial y_I}\dot{y}_I\right\} = 0 \tag{2.9a}$$

under boundary conditions

$$V(x_1, y_1, \dots, x_n, y_n, x_I, y_I) = 0 \tag{2.9b}$$

$$\phi(x_I, y_I) = 0 \tag{2.9c}$$

$$\min_{j=1,\dots,n}\{(x_j - x_I)^2 + (y_j - y_I)^2\} = r. \tag{2.9d}$$

The boundary condition is built from the following facts. When the initial location of the invader is at the boundary of the target (Eq. (2.9c)) and there is at least one defender within the capture range (Eq (2.9d)), the invader will be captured immediately (Eq. (2.9b)).

Clearly, the geometric solution satisfies the boundary condition, because $\mathcal{D}_I$ reduces to $\boldsymbol{p}^*$, thereby $V^g = g(x_I^*, y_I^*) = 0$. So the core task of this paper is to prove V^g satisfies (2.9a).

3. Proof for the SDSI game

3.1. Notations

Since SDSI game is a special case of the MDSI game, this section adopts a simplified notation as listed in Table 1. In addition, we will need another function, the slope of $\partial\mathcal{D}_I$, denoted by $k(x, y, x_D, y_D, x_I, y_I)$. By definition, the function of $\partial\mathcal{D}_I$ is

$$d(x, y, x_D, y_D, x_I, y_I) = 0. \tag{3.1}$$

For fixed x_D, y_D, x_I, y_I, (3.1) is an implicit function of $y(x)$. Taking the derivative of (3.1) over x gives

$$d_x(x, y, x_D, y_D, x_I, y_I) + d_y(x, y, x_D, y_D, x_I, y_I)\frac{dy}{dx} = 0, \tag{3.2}$$

where $d_x = \partial d/\partial x$, $d_y = \partial d/\partial y$. Then,

$$k(x, y, x_D, y_D, x_I, y_I) := \frac{dy}{dx} = -\frac{d_x(x, y, x_D, y_D, x_I, y_I)}{d_y(x, y, x_D, y_D, x_I, y_I)}. \tag{3.3}$$

In the proof, we will be handling partial derivatives of ϕ, d, k, x^*, y^*, V, V^g. For simplicity, we put the variable w.r.t. which the partial derivative is taken as the subscript. For example, $\partial\phi/\partial x$ is denoted for short as ϕ_x. In addition, define

$$\cos\alpha(x, y) = \frac{x - x_D}{R_D(x, y)}, \qquad \sin\alpha(x, y) = \frac{y - y_D}{R_D(x, y)}, \tag{3.4a}$$

$$\cos\beta(x, y) = \frac{x - x_I}{R_I(x, y)}, \qquad \sin\beta(x, y) = \frac{y - y_I}{R_I(x, y)}, \tag{3.4b}$$

$$\rho_D = \frac{a\cos(\alpha - \beta) - 1}{(d_y)^2 R_D}, \qquad \rho_I = \frac{\cos(\alpha - \beta) - a}{(d_y)^2 R_I}, \tag{3.5}$$

$$\begin{aligned} \boldsymbol{e}_\alpha &= [\cos\alpha, \sin\alpha]^T, \quad \tilde{\boldsymbol{e}}_\alpha = [\sin\alpha, \cos\alpha]^T, \\ \boldsymbol{e}_\beta &= [\cos\beta, \sin\beta]^T, \quad \tilde{\boldsymbol{e}}_\beta = [\sin\beta, \cos\beta]^T. \end{aligned} \tag{3.6}$$

Among the notations above, ϕ, d, k, R_D, R_I, α, β, ρ_D, ρ_I, $\boldsymbol{e}_\alpha$, $\boldsymbol{e}_\beta$, $\tilde{\boldsymbol{e}}_\alpha$, $\tilde{\boldsymbol{e}}_\beta$ are functions whose arguments contain x, y. These functions will be evaluated at $x = x^*$, $y = y^*$. This is emphasized through subscript/superscript $*$, as shown in Table 2.

Table 1
Correlations of the notations for the MDSI and the SDSI game.

For D_j in MDSI Game	For D in SDSI Game
$\boldsymbol{p}_j = [x_j, y_j]^T$, $P_{aux}(D_j)$	$\boldsymbol{p}_D = [x_D, y_D]^T$, $P_{aux}(D)$
$\mathcal{D}_I^j$, $\partial\mathcal{D}_I^j$, $R_j(x, y)$	$\mathcal{D}_I$, $\partial\mathcal{D}_I$, $R_D(x, y)$
$d^j(x, y, x_j, y_j, x_I, y_I)$	$d(x, y, x_D, y_D, x_I, y_I)$
$\boldsymbol{v}_j^g(x_1, y_1, \ldots, x_n, y_n, x_I, y_I)$	$\boldsymbol{v}_D^g(x_D, y_D, x_I, y_I)$
$V^g(x_1, y_1, \ldots, x_n, y_n, x_I, y_I)$	$V^g(x_D, y_D, x_I, y_I)$

Table 2
Notations for functions at $[x^*, y^*]^T$.

Functions	Functions at $x = x^*$, $y = y^*$
ϕ_x, ϕ_y, ϕ_{xx}, ϕ_{xy}, ϕ_{yx}, g_{yy}	ϕ_{x^*}, ϕ_{y^*}, ϕ_{xx^*}, ϕ_{xy^*}, ϕ_{yx^*}, ϕ_{yy^*}
d_x, d_y, d_{x_D}, d_{y_D}, d_{x_I}, d_{y_I}	d_{x^*}, d_{y^*}, $d_{x_D}^*$, $d_{y_D}^*$, $d_{x_I}^*$, $d_{y_I}^*$
k_x, k_y, k_{x_D}, k_{y_D}, k_{x_I}, k_{y_I}	k_{x^*}, k_{y^*}, $k_{x_D}^*$, $k_{y_D}^*$, $k_{x_I}^*$, $k_{y_I}^*$
d, k, ϕ R_D, R_I, ρ_D, ρ_I	d_*, k_*, ϕ_*, R_D^*, R_I^*, ρ_D^*, ρ_I^*
α, β, $\boldsymbol{e}_\alpha$, $\boldsymbol{e}_\beta$, $\tilde{\boldsymbol{e}}_\alpha$, $\tilde{\boldsymbol{e}}_\beta$	α^*, β^*, $\boldsymbol{e}_{\alpha^*}$, $\boldsymbol{e}_{\beta^*}$, $\tilde{\boldsymbol{e}}_{\alpha^*}$, $\tilde{\boldsymbol{e}}_{\beta^*}$

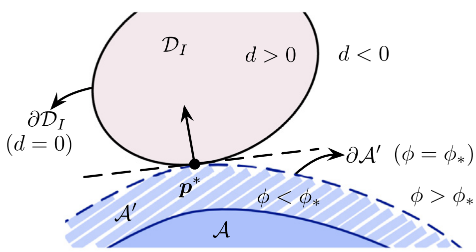

Fig. 3. Proof for Lemma 3.1.

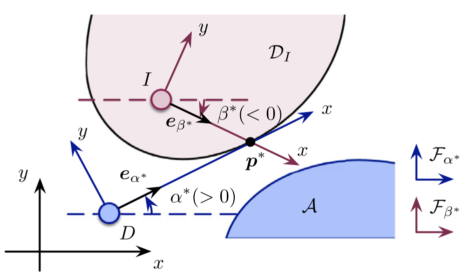

Fig. 4. Definitions of $\mathcal{F}_{\alpha^*}$ and $\mathcal{F}_{\beta^*}$.

Lemma 3.1. *For the SDSI game with dynamics (2.2), target area (2.1), and assumptions A1–A5, we have*

$$\frac{\phi_{x^*}}{\phi_{y^*}} = \frac{d_{x^*}}{d_{y^*}} > 0. \tag{3.7}$$

Proof. According to convex optimization theory, $\partial\mathcal{D}_I$ is tangent to contour $\partial\mathcal{A}' = \{[x, y]^T | \phi(x, y) = \phi_*\}$ at $\boldsymbol{p}^* = [x^*, y^*]^T$, as shown in Fig. 3. Hence the gradient of d and ϕ at $\boldsymbol{p}^*$, namely $[\phi_{x^*}, \phi_{y^*}]^T$ and $[d_{x^*}, d_{y^*}]^T$ must be parallel. By definitions of ϕ, d, both d and ϕ increase along the direction from $\boldsymbol{p}^*$ pointing into the dominance region. So $[\phi_{x^*}, \phi_{y^*}]^T$ and $[d_{x^*}, d_{y^*}]^T$ are along the same direction. This implies (3.7). □

In the end, define frame $\mathcal{F}_{\alpha^*}$ s.t. its x-axis is along $\boldsymbol{e}_{\alpha^*}$. Similarly, define $\mathcal{F}_{\beta^*}$ whose x-axis is along $\boldsymbol{e}_{\beta^*}$, as shown in Fig. 4.

3.2. Overview of the proof

Let $\partial_{\boldsymbol{p}_D} V = [V_{x_D}, V_{y_D}]^T$, $\partial_{\boldsymbol{p}_I} V = [V_{x_I}, V_{y_I}]^T$, the HJI equation (2.9a) can be re-organized as

$$\min_{\boldsymbol{v}_I} \max_{\boldsymbol{v}_D} \left\{ (\partial_{\boldsymbol{p}_D} V)^T \boldsymbol{v}_D + (\partial_{\boldsymbol{p}_I} V)^T \boldsymbol{v}_I \right\} = 0. \tag{3.8}$$

Lemma 3.2. *For control laws $\boldsymbol{v}_D$, $\boldsymbol{v}_I$, and function V to solve HJI equation (3.8), it must be satisfied that*

$$\boldsymbol{v}_D = v_D \frac{\partial_{\boldsymbol{p}_D} V}{\|\partial_{\boldsymbol{p}_D} V\|}, \quad \boldsymbol{v}_I = -v_I \frac{\partial_{\boldsymbol{p}_I} V}{\|\partial_{\boldsymbol{p}_I} V\|}, \tag{3.9a}$$

$$a\|\partial_{\boldsymbol{p}_D} V\| = \|\partial_{\boldsymbol{p}_I} V\|. \tag{3.9b}$$

To verify (3.9), we need to calculate $\partial_{\boldsymbol{p}_D} V^g$, $\partial_{\boldsymbol{p}_I} V^g$. Recall $V^g = g(x^*, y^*)$ and use the chain rule,

$$\partial_{\boldsymbol{p}_D} V^g = \begin{bmatrix} V_{x_D}^g \\ V_{y_D}^g \end{bmatrix} = \begin{bmatrix} x_{x_D}^* \phi_{x^*} + y_{x_D}^* \phi_{y^*} \\ x_{y_D}^* \phi_{x^*} + y_{y_D}^* \phi_{y^*} \end{bmatrix}, \tag{3.10a}$$

$$\partial_{\boldsymbol{p}_I} V^g = \begin{bmatrix} V_{x_I}^g \\ V_{y_I}^g \end{bmatrix} = \begin{bmatrix} x_{x_I}^* \phi_{x^*} + y_{x_I}^* \phi_{y^*} \\ x_{y_I}^* \phi_{x^*} + y_{y_I}^* \phi_{y^*} \end{bmatrix}. \tag{3.10b}$$

$x_{x_D}^*$, $x_{y_D}^*$, $y_{x_D}^*$, $y_{y_D}^*$, $x_{x_I}^*$, $x_{y_I}^*$, $y_{x_I}^*$, $y_{y_I}^*$ can be computed by converting $P_{aux}(D)$ into an implicit function of $x^*(x_D, y_D, x_I, y_I)$, $y^*(x_D, y_D, x_I, y_I)$. An overview of the proof is presented below.

I Construct an implicit function of $x^*(x_D, y_D, x_I, y_I)$, $y^*(x_D, y_D, x_I, y_I)$ using $P_{aux}(D)$.
II Compute $x_{x_D}^*$, $x_{y_D}^*$, $x_{x_I}^*$, $x_{y_I}^*$, $y_{x_D}^*$, $y_{y_D}^*$, $y_{x_I}^*$, $y_{y_I}^*$ by taking derivatives of the implicit function constructed in step I.
III Use the chain rule (3.10) and the derivatives computed in step II to compute $\partial_{\boldsymbol{p}_D} V^g$ and $\partial_{\boldsymbol{p}_I} V^g$.
IV Verify $\partial_{\boldsymbol{p}_D} V^g$, $\partial_{\boldsymbol{p}_I} V^g$ and the geometric control law (2.7) using Lemma 3.2.

3.3. Details of the proof

3.3.1. Step I: Construct the implicit function of x^* and y^*

Lemma 3.3. *Under A5, a necessary condition for $[x^*, y^*]^T$ to solve $P_{aux}(D)$ is to satisfy Eq. (3.11).*

$$\phi_{x^*} + \phi_{y^*} k(x^*, y^*, x_D, y_D, x_I, y_I) = 0, \tag{3.11a}$$

$$d(x^*, y^*, x_D, y_D, x_I, y_I) = 0. \tag{3.11b}$$

Proof. Under A5, $[x^*, y^*]^T \in \partial\mathcal{D}_I$, which gives (3.11b). This also converts the constraint of $P_{aux}(D)$ as $d(x, y, x_D, y_D, x_I, y_I) = 0$. For given x_D, y_D, x_I, y_I, $d(x, y, x_D, y_D, x_I, y_I) = 0$ can be viewed as an implicit function of $y(x)$. By substituting $y(x)$ into ϕ, $P_{aux}(D)$ becomes an unconstrained optimization problem regarding x only. A necessary condition for x to be the solution of $P_{aux}(D)$ is $d\phi/dx = 0$, which expands as

$$\frac{d\phi(x, y(x))}{dx} = \phi_x(x, y(x)) + \phi_y(x, y(x)) k(x, y(x), x_D, y_D, x_I, y_I) = 0. \tag{3.12}$$

Replacing x, $y(x)$ with x^*, y^* in (3.12) gives (3.11a). □

3.3.2. Step II, compute partial derivatives of x^*, y^*

Taking derivatives of (3.11) over x_D gives

$$\begin{aligned} &\phi_{xx^*} x_{x_D}^* + \phi_{xy^*} y_{x_D}^* + \left(\phi_{yx^*} x_{x_D}^* + \phi_{yy^*} y_{x_D}^*\right) k_* + \\ &\qquad \phi_{y^*} \left(k_{x^*} x_{x_D}^* + k_{y^*} y_{x_D}^* + k_{x_D}^*\right) = 0, \\ &\qquad d_{x^*} x_{x_D}^* + d_{y^*} y_{x_D}^* + d_{x_D}^* = 0. \end{aligned} \tag{3.13}$$

This is a linear equation regarding $x_{x_D}^*$, $y_{x_D}^*$, thus can be solved directly. The same process can be executed for y_D, x_I, y_I. After this, we can substitute the detailed expressions of d, k and their derivatives into the result, and simplify the representation using

$\boldsymbol{e}_{\alpha*}$, $\boldsymbol{e}_{\beta*}$, $\tilde{\boldsymbol{e}}_{\alpha*}$, $\tilde{\boldsymbol{e}}_{\beta*}$ and the auxiliary variables defined in (3.14).

$$\begin{aligned} K_* &= [1, k_*]^T, \quad \nabla\phi_* = [\phi_{x*}, \phi_{y*}]^T, \\ \nabla\phi_{x*} &= [\phi_{xx*}, \phi_{yx*}]^T, \quad \nabla\phi_{y*} = [\phi_{xy*}, \phi_{yy*}]^T, \\ R_+ &= \begin{bmatrix} \rho_D^* & 0 \\ 0 & \rho_I^* \end{bmatrix}, \quad R_- = \begin{bmatrix} \rho_D^* & 0 \\ 0 & -\rho_I^* \end{bmatrix}, \\ \Delta &= \text{Determinant of (3.13)}. \end{aligned} \tag{3.14}$$

The result is presented in Eq. (3.15). Exemplar derivations for (3.15a), (3.15b) can be found in Appendix B.1.

$$x^*_{x_D} = -K_*^T \nabla\phi_{y*} \cos\alpha^*/\Delta + \left(\rho_D^* - a\tilde{\boldsymbol{e}}^T_{\alpha*} R_- \tilde{\boldsymbol{e}}_{\beta*}\right)\phi_{y*}/\Delta, \tag{3.15a}$$

$$y^*_{x_D} = K_*^T \nabla\phi_{x*} \cos\alpha^*/\Delta + \left(a\tilde{\boldsymbol{e}}^T_{\alpha*} R_+ \boldsymbol{e}_{\beta*}\right)\phi_{y*}/\Delta, \tag{3.15b}$$

$$x^*_{y_D} = -K_*^T \nabla\phi_{y*} \sin\alpha^*/\Delta + \left(a\boldsymbol{e}^T_{\alpha*} R_+ \tilde{\boldsymbol{e}}_{\beta*}\right)\phi_{y*}/\Delta, \tag{3.15c}$$

$$y^*_{y_D} = K_*^T \nabla\phi_{x*} \sin\alpha^*/\Delta + \left(\rho_D^* - a\boldsymbol{e}^T_{\alpha*} R_- \boldsymbol{e}_{\beta*}\right)\phi_{y*}/\Delta, \tag{3.15d}$$

$$x^*_{x_I} = aK_*^T \nabla\phi_{y*} \cos\beta^*/\Delta - \left(a^2\rho_I^* + a\boldsymbol{e}^T_{\alpha*} R_- \boldsymbol{e}_{\beta*}\right)\phi_{y*}/\Delta, \tag{3.15e}$$

$$y^*_{x_I} = -aK_*^T \nabla\phi_{x*} \cos\beta^*/\Delta - \left(a\tilde{\boldsymbol{e}}^T_{\alpha*} R_+ \boldsymbol{e}_{\beta*}\right)\phi_{y*}/\Delta, \tag{3.15f}$$

$$x^*_{y_I} = aK_*^T \nabla\phi_{y*} \sin\beta^*/\Delta - \left(a\boldsymbol{e}^T_{\alpha*} R_+ \tilde{\boldsymbol{e}}_{\beta*}\right)\phi_{y*}/\Delta, \tag{3.15g}$$

$$y^*_{y_I} = -aK_*^T \nabla\phi_{x*} \sin\beta^*/\Delta - \left(a^2\rho_I^* + a\tilde{\boldsymbol{e}}^T_{\alpha*} R_- \tilde{\boldsymbol{e}}_{\beta*}\right)\phi_{y*}/\Delta. \tag{3.15h}$$

Remark 3.1. Eq. (3.15) is not well-defined when $\Delta = 0$, however, Δ will be canceled out in $\partial_{\boldsymbol{p}_D} V^g$, $\partial_{\boldsymbol{p}_I} V^g$.

3.3.3. Step III: Compute $\partial_{\boldsymbol{p}_D} V^g$, $\partial_{\boldsymbol{p}_I} V^g$

Substituting Eqs. (3.15a)–(3.15d) into (3.10a), we have

$$\begin{aligned} \partial_{\boldsymbol{p}_D} V^g = &- K_*^T \nabla\phi_{y*}\phi_{x*} \begin{bmatrix} \cos\alpha^* \\ \sin\alpha^* \end{bmatrix} /\Delta + K_*^T \nabla\phi_{x*}\phi_{y*} \begin{bmatrix} \cos\alpha^* \\ \sin\alpha^* \end{bmatrix} /\Delta + \\ &\phi_{x*}\phi_{y*} \begin{bmatrix} \rho_D^* - a\tilde{\boldsymbol{e}}^T_{\alpha*} R_- \tilde{\boldsymbol{e}}_{\beta*} \\ a\boldsymbol{e}^T_{\alpha*} R_+ \tilde{\boldsymbol{e}}_{\beta*} \end{bmatrix} /\Delta \\ &+ \phi_{y*}^2 \begin{bmatrix} a\tilde{\boldsymbol{e}}^T_{\alpha*} R_+ \boldsymbol{e}_{\beta*} \\ \rho_D^* - a\boldsymbol{e}^T_{\alpha*} R_- \boldsymbol{e}_{\beta*} \end{bmatrix} /\Delta. \end{aligned} \tag{3.16}$$

It can be seen that the first two terms are along $\boldsymbol{e}_{\alpha*}$, so we attempt to write the other two terms in frame $\mathcal{F}_{\alpha*}$ as well. Let

$$\boldsymbol{\gamma}_D^1 = \begin{bmatrix} \rho_D^* - a\tilde{\boldsymbol{e}}^T_{\alpha*} R_- \tilde{\boldsymbol{e}}_{\beta*} \\ a\boldsymbol{e}^T_{\alpha*} R_+ \tilde{\boldsymbol{e}}_{\beta*} \end{bmatrix} /\Delta, \quad \boldsymbol{\gamma}_D^2 = \begin{bmatrix} a\tilde{\boldsymbol{e}}^T_{\alpha*} R_+ \boldsymbol{e}_{\beta*} \\ \rho_D^* - a\boldsymbol{e}^T_{\alpha*} R_- \boldsymbol{e}_{\beta*} \end{bmatrix} /\Delta, \tag{3.17}$$

then the coordinates of $\boldsymbol{\gamma}_D^1$, $\boldsymbol{\gamma}_D^2$ in $\mathcal{F}_{\alpha*}$ can be computed through their dot and cross products with $\boldsymbol{e}_{\alpha*}$:

$$\left[\boldsymbol{\gamma}_D^1\right]_{\mathcal{F}_{\alpha*}} = \begin{bmatrix} \boldsymbol{e}_{\alpha*} \cdot \boldsymbol{\gamma}_D^1 \\ \boldsymbol{e}_{\alpha*} \times \boldsymbol{\gamma}_D^1 \end{bmatrix}, \quad \left[\boldsymbol{\gamma}_D^2\right]_{\mathcal{F}_{\alpha*}} = \begin{bmatrix} \boldsymbol{e}_{\alpha*} \cdot \boldsymbol{\gamma}_D^2 \\ \boldsymbol{e}_{\alpha*} \times \boldsymbol{\gamma}_D^2 \end{bmatrix}. \tag{3.18}$$

Substituting the definitions of $\boldsymbol{e}_{\alpha*}$, $\boldsymbol{\gamma}_D^1$, $\boldsymbol{\gamma}_D^2$, the result yields

$$\left[\boldsymbol{\gamma}_D^1\right]_{\mathcal{F}_{\alpha*}} = -\begin{bmatrix} k_{y*} \\ \rho_D^* d_{y*} \end{bmatrix} /\Delta, \quad \left[\boldsymbol{\gamma}_D^2\right]_{\mathcal{F}_{\alpha*}} = \begin{bmatrix} k_{x*} \\ \rho_D^* d_{x*} \end{bmatrix} /\Delta. \tag{3.19}$$

Detailed computations can be found in Appendix B.3. Then, Eq. (3.16) becomes

$$\begin{aligned} \partial_{\boldsymbol{p}_D} V^g &= K_*^T\left(-\nabla\phi_{y*}\phi_{x*} + \nabla\phi_{x*}\phi_{y*}\right)\boldsymbol{e}_{\alpha*}/\Delta + \phi_{x*}\phi_{y*}\boldsymbol{\gamma}_D^1 + \phi_{y*}^2\boldsymbol{\gamma}_D^2 \\ &= \phi_{y*}K_*^T\left(-\nabla\phi_{y*}\frac{\phi_{x*}}{\phi_{y*}} + \nabla\phi_{x*}\right)\boldsymbol{e}_{\alpha*}/\Delta + \phi_{y*}^2\left(\frac{\phi_{x*}}{\phi_{y*}}\boldsymbol{\gamma}_D^1 + \boldsymbol{\gamma}_D^2\right) \\ &= \phi_{y*}K_*^T\left(\nabla\phi_{y*}k_* + \nabla\phi_{x*}\right)\boldsymbol{e}_{\alpha*}/\Delta + \phi_{y*}^2\left(-k_*\boldsymbol{\gamma}_D^1 + \boldsymbol{\gamma}_D^2\right) \\ &= \phi_{y*}\left(K_*^T H_{\phi_*} K_*\right)\boldsymbol{e}_{\alpha*}/\Delta - k_*\phi_{y*}^2\boldsymbol{\gamma}_D^1 + \phi_{y*}^2\boldsymbol{\gamma}_D^2, \end{aligned}$$

where $H_{\phi_*} = [\nabla\phi_{x*}, \nabla\phi_{y*}]$ is the Hessian of ϕ at $[x^*, y^*]^T$. Now, express $\boldsymbol{\gamma}_D^1$, $\boldsymbol{\gamma}_D^2$, $\boldsymbol{e}_{\alpha*}$ in $\mathcal{F}_{\alpha*}$, the coordinate of $\partial_{\boldsymbol{p}_D} V$ becomes

$$\begin{aligned} \left[\partial_{\boldsymbol{p}_D} V^g\right]_{\mathcal{F}_{\alpha*}} &= \frac{1}{\Delta}\left(\begin{bmatrix} \phi_{y*}K_*^T H_{\phi_*} K_* \\ 0 \end{bmatrix}\right. \\ &\quad \left. + k_*\phi_{y*}^2 \begin{bmatrix} k_{y*} \\ \rho_D^* d_{y*} \end{bmatrix} + \phi_{y*}^2 \begin{bmatrix} k_{x*} \\ \rho_D^* d_{x*} \end{bmatrix}\right) \\ &= \frac{\phi_{y*}}{\Delta}\begin{bmatrix} K_*^T H_{\phi_*} K_* + \phi_{y*}(k_* k_{y*} + k_{x*}) \\ \rho_D^*(k_* d_{y*} + d_{x*})\phi_{y*} \end{bmatrix}. \end{aligned}$$

Since $d_{x*}/d_{y*} = -k_*$, the second component of $[\partial_{\boldsymbol{p}_D} V]_{\mathcal{F}_{\alpha*}}$ is 0. Also, it can be proved that

$$K_*^T H_{\phi_*} K_* + \phi_{y*}(k_* k_{y*} + k_{x*}) = \Delta/d_{y*}. \tag{3.20}$$

See Eq. (B.5), Appendix B.2. As a result,

$$\left[\partial_{\boldsymbol{p}_D} V^g\right]_{\mathcal{F}_{\alpha*}} = \begin{bmatrix} \phi_{y*}/d_{y*} \\ 0 \end{bmatrix}. \tag{3.21a}$$

Following a similar process (a sketch can be found in Appendix B.4), the coordinate of $\partial_{\boldsymbol{p}_I} V$ in $\mathcal{F}_{\beta*}$ turns out to be

$$\left[\partial_{\boldsymbol{p}_I} V^g\right]_{\mathcal{F}_{\beta*}} = -a\begin{bmatrix} \phi_{y*}/d_{y*} \\ 0 \end{bmatrix}. \tag{3.21b}$$

3.3.4. Step IV: Verify the geometric solution using Lemma 3.2

Compare (3.21a) (3.21b) with Eq. (3.9) and use the definition of $\mathcal{F}_{\alpha*}$, $\mathcal{F}_{\beta*}$, it can be seen that Lemma 3.2 is satisfied if $\phi_{y*}/d_{y*} > 0$, which is guaranteed by Lemma 3.1. Further, since ϕ, d are second-order differentiable, ϕ is convex, d is concave, and $[x^*, y^*]^T$ is not an extremum of d, thus ϕ_{y*}/d_{y*} must be finite. This means V^g is differentiable, thereby is the classic solution of the HJI equation.

Remark 3.2. (3.13) is only a necessary condition. In fact, it has another solution which maximizes ϕ. These two solutions are distinguished by the sign of ϕ_{y*}/d_{y*}. If $\boldsymbol{p}^*$ maximized ϕ, then $\phi_{y*}/d_{y*} < 0$, the HJI equation would not be satisfied.

4. Proof for the MDSI game

This section starts with the 2DSI game, the proof for the MDSI game is a direct extension.

4.1. Notations in the 2DSI game

Here we use the MDSI notations from Table 1. In addition, the definition of α is extended into $\alpha_j, j = 1, 2$ by replacing all the subscript D with $j = 1, 2$ in Eq. (3.4). The definitions of $\boldsymbol{e}_\alpha$, $\tilde{\boldsymbol{e}}_\alpha$ are extended into $\boldsymbol{e}_j$, $\tilde{\boldsymbol{e}}_j, j = 1, 2$ accordingly. Here we discuss three games, the SDSI game between the invader and each defender, and the 2DSI game among all the three players. Let $\boldsymbol{p}_1^*$, $\boldsymbol{p}_2^*$ and $\boldsymbol{p}^*$ be the solutions to their auxiliary problems. In addition, consider the closer intersection of $\partial\mathcal{D}_I^1$, $\partial\mathcal{D}_I^2$, denoted by $\boldsymbol{p}^\star = [x^\star, y^\star]^T$. Similar to how $\boldsymbol{p}^*$ is handled in the SDSI game, we will compute derivatives of $x^\star$, $y^\star$ w.r.t. player locations, including $x^\star_{x_j}$, $y^\star_{x_j}$, $x^\star_{y_j}$, $y^\star_{y_j}$, $j = 1, 2$, and $x^\star_{x_I}$, $x^\star_{y_I}$, $y^\star_{x_I}$, $y^\star_{y_I}$. When a function is evaluated at $\boldsymbol{p}^\star$, a subscript $\star$ is added, the same way as $*$ is used in Table 2.

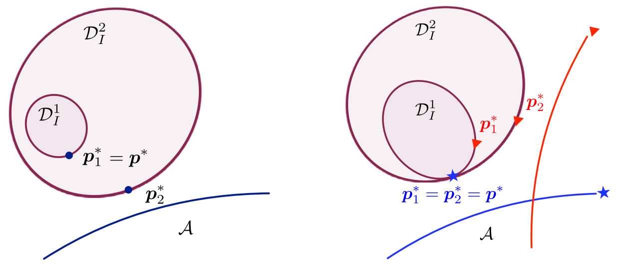

(a) $\partial\mathcal{D}_I^1 \cap \partial\mathcal{D}_I^2 = \emptyset$ (b) $\partial\mathcal{D}_I^1 \cap \partial\mathcal{D}_I^2 \neq \emptyset$

Fig. 5. Relationship of $\mathcal{D}_I^1$, $\mathcal{D}_I^2$: one belongs to the other. As an example, $\mathcal{D}_I^1 \subseteq \mathcal{D}_I^2$.

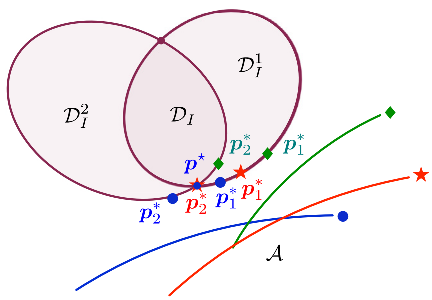

Fig. 6. Relationship of $\mathcal{D}_I^1$, $\mathcal{D}_I^2$: neither belongs to the other. (For interpretation of the references to color in this figure legend, the reader is referred to the web version of this article.)

4.2. Degeneration of the 2DSI game

The 2DSI game degenerates into an SDSI game in most situations. This can be identified through enumeration. First of all, the two dominance regions $\mathcal{D}_I^1$, $\mathcal{D}_I^2$ must intersect because they have at least one common point, the invader. As a result, the relationship between $\mathcal{D}_I^1$ and $\mathcal{D}_I^2$ has two possibilities, one belongs to the other, or neither belongs to the other. If the former is true (see Fig. 5), the game is degenerated, because the intersection of the two dominance regions is equal to the smaller one. If neither of $\mathcal{D}_I^1$, $\mathcal{D}_I^2$ belongs to the other, whether the game is degenerated is determined by the target area. As shown in Fig. 6, when the target area is at the blue (dot) position, the solution of $P_{aux}(D_1, D_2)$ is distinct from both $\boldsymbol{p}_1^*$, $\boldsymbol{p}_2^*$. Instead, it is at $\boldsymbol{p}^\star$. If the two defenders both move toward $\boldsymbol{p}^\star$, the invader can be captured at a further distance from the target than in any of the SDSI games, thus the 2DSI game is not degenerated. In fact, this is the only non-degenerated case. When the target area is at the green (diamond) location, the game degenerates as an SDSI game with D_2. In between the blue (dot) and green (diamond) locations is the critical condition where $\boldsymbol{p}_2^* = \boldsymbol{p}^\star$ (red, star), which can be viewed as both a 2DSI and an SDSI game.

4.3. Proof for the non-degenerated 2DSI game

This proof follows the same procedure as the SDSI game. Firstly, let $\partial_{\boldsymbol{p}_1} V = [V_{x_1}, V_{y_1}]^T$, $\partial_{\boldsymbol{p}_2} V = [V_{x_2}, V_{y_2}]^T$, $\partial_{\boldsymbol{p}_I} V = [V_{x_I}, V_{y_I}]^T$, and re-organize the HJI equation (2.9a) as

$$\min_{\boldsymbol{v}_I} \max_{\boldsymbol{v}_1,\boldsymbol{v}_2} \left\{ (\partial_{\boldsymbol{p}_1} V)^T \boldsymbol{v}_1 + (\partial_{\boldsymbol{p}_2} V)^T \boldsymbol{v}_2 + (\partial_{\boldsymbol{p}_I} V)^T \boldsymbol{v}_I \right\} = 0. \tag{4.1}$$

Lemma 4.1. *For control laws $\boldsymbol{v}_1$, $\boldsymbol{v}_2$, $\boldsymbol{v}_I$, and function V to solve HJI equation (4.1), it must be satisfied that*

$$\begin{aligned} &\boldsymbol{v}_1 = v_D \frac{\partial_{\boldsymbol{p}_1} V}{\|\partial_{\boldsymbol{p}_1} V\|}, \quad \boldsymbol{v}_2 = v_D \frac{\partial_{\boldsymbol{p}_2} V}{\|\partial_{\boldsymbol{p}_2} V\|}, \quad \boldsymbol{v}_I = -v_I \frac{\partial_{\boldsymbol{p}_I} V}{\|\partial_{\boldsymbol{p}_I} V\|}, \\ &a\|\partial_{\boldsymbol{p}_1} V\| + a\|\partial_{\boldsymbol{p}_2} V\| = \|\partial_{\boldsymbol{p}_I} V\|. \end{aligned} \tag{4.2}$$

The implicit function of $x^\star$, $y^\star$ is given by

$$\begin{cases} d^1(x^\star, y^\star, x_1, y_1, x_I, y_I) = 0 \\ d^2(x^\star, y^\star, x_2, y_2, x_I, y_I) = 0 \end{cases}. \tag{4.3}$$

Differentiating (4.3) w.r.t. x_1 gives

$$\begin{aligned} d^1_{x^\star} x^\star_{x_1} + d^1_{y^\star} y^\star_{x_1} + d^1_{x_1^\star} &= 0, \\ d^2_{x^\star} x^\star_{x_1} + d^2_{y^\star} y^\star_{x_1} &= 0, \end{aligned} \tag{4.4}$$

from which it can be solved that

$$x^\star_{x_1} = d^1_{x_1^\star} d^2_{y^\star} / \Omega, \qquad y^\star_{x_1^\star} = -d^1_{x_1} d^2_{x^\star} / \Omega, \tag{4.5}$$

where $\Omega = d^1_{y^\star} d^2_{x^\star} - d^1_{x^\star} d^2_{y^\star}$ is the determinant of (4.4). Repeating this for y_1, x_2, y_2, x_I, y_I gives

$$\begin{aligned} x^\star_{x_1} &= -\cos\alpha_{1\star} d^2_{y^\star}/\Omega, & y^\star_{x_1} &= \cos\alpha_{1\star} d^2_{x^\star}/\Omega, \\ x^\star_{y_1} &= -\sin\alpha_{1\star} d^2_{y^\star}/\Omega, & y^\star_{y_1} &= \sin\alpha_{1\star} d^2_{x^\star}/\Omega, \\ x^\star_{x_2} &= \cos\alpha_{2\star} d^1_{y^\star}/\Omega, & y^\star_{x_2} &= -\cos\alpha_{2\star} d^1_{x^\star}/\Omega, \\ x^\star_{y_2} &= \sin\alpha_{2\star} d^1_{y^\star}/\Omega, & y^\star_{y_2} &= -\sin\alpha_{2\star} d^1_{x^\star}/\Omega, \\ x^\star_{x_I} &= a\cos\beta_\star (d^2_{y^\star} - d^1_{y^\star})/\Omega, & y^\star_{x_I} &= -a\cos\beta_\star (d^2_{x^\star} - d^1_{x^\star})/\Omega, \\ x^\star_{y_I} &= a\sin\beta_\star (d^2_{y^\star} - d^1_{y^\star})/\Omega, & y^\star_{y_I} &= -a\sin\beta_\star (d^2_{x^\star} - d^1_{x^\star})/\Omega. \end{aligned} \tag{4.6}$$

Then, $\partial_{\boldsymbol{p}_1} V^g$ can be computed using the chain rule:

$$\begin{aligned} \partial_{\boldsymbol{p}_1} V^g &= \begin{bmatrix} g_{x^\star} x^\star_{x_1} + g_{y^\star} y^\star_{x_1} \\ g_{x^\star} x^\star_{y_1} + g_{y^\star} y^\star_{y_1} \end{bmatrix} \\ &= \begin{bmatrix} -\cos\alpha_{1\star} g_{x^\star} d^2_{y^\star} + \cos\alpha_{1\star} g_{y^\star} d^2_{x^\star} \\ -\sin\alpha_{1\star} g_{x^\star} d^2_{y^\star} + \sin\alpha_{1\star} g_{y^\star} d^2_{x^\star} \end{bmatrix} / \Omega \\ &= \left(-g_{x^\star} d^2_{y^\star} + g_{y^\star} d^2_{x^\star}\right) \begin{bmatrix} \cos\alpha_{1\star} \\ \sin\alpha_{1\star} \end{bmatrix} / \Omega. \end{aligned}$$

$\partial_{\boldsymbol{p}_2} V^g$, $\partial_{\boldsymbol{p}_I} V^g$ can be computed in the same way. Let $\nabla g_\star = [g_{x^\star}, g_{y^\star}]^T$, $\nabla d^j_\star = [d^j_{x^\star}, d^j_{y^\star}]^T$, $j = 1, 2$, $\Omega = \nabla d^1_\star \times \nabla d^2_\star$, we have

$$\begin{aligned} \partial_{\boldsymbol{p}_1} V^g &= -\left(\nabla g_\star \times \nabla d^2_\star\right) \boldsymbol{e}_{1\star}/\Omega, \\ \partial_{\boldsymbol{p}_2} V^g &= \left(\nabla g_\star \times \nabla d^1_\star\right) \boldsymbol{e}_{2\star}/\Omega, \\ \partial_{\boldsymbol{p}_I} V^g &= a\left(\nabla g_\star \times \nabla d^2_\star - \nabla g_\star \times \nabla d^1_\star\right) \boldsymbol{e}_{\beta^\star}/\Omega. \end{aligned} \tag{4.7}$$

To determine signs of the cross products in (4.7), assume $\mathcal{D}_I^1$ is on the right, see Fig. 7. Since $\boldsymbol{p}^\star \neq \boldsymbol{p}_j^*$, ϕ must decrease along the tangent vector of $\partial\mathcal{D}_I^1$ at $\boldsymbol{p}^\star$, denoted by $\boldsymbol{t}_1$. Similarly, ϕ also decreases along $-\boldsymbol{t}_2$. Note $\nabla d^j_\star$ is perpendicular to $\boldsymbol{t}_j$ and points into the dominance region, therefore $\nabla g_\star$ must be between $\nabla d^1_\star$ and $\nabla d^2_\star$. Then it can be asserted that $\nabla g_\star \times \nabla d^1_\star < 0$, $\nabla g_\star \times \nabla d^2_\star > 0$ and $\nabla d^2_\star \times \nabla d^1_\star < 0$. Using this in (4.7) gives $\partial_{\boldsymbol{p}_1} V > 0$, $\partial_{\boldsymbol{p}_2} V > 0$, $\partial_{\boldsymbol{p}_I} V < 0$. This makes Lemma 4.1 satisfied.

It can be further proved that $\partial_{\boldsymbol{p}_1} V^g$, $\partial_{\boldsymbol{p}_2} V^g$, $\partial_{\boldsymbol{p}_I} V^g$ are finite. This is apparent when $\partial\mathcal{D}_I^1$, $\partial\mathcal{D}_I^2$ intersect at $\boldsymbol{p}^\star$, since $\nabla d^1_\star$, $\nabla d^2_\star$ are not parallel thus $\Omega \neq 0$. When $\partial\mathcal{D}_I^1$, $\partial\mathcal{D}_I^2$ are tangent at $\boldsymbol{p}^\star$, $\nabla g_\star$, $\nabla d^1_\star$, $\nabla d^2_\star$ become colinear, so we need to investigate the limit of (4.7). Because $\nabla g_\star$, $\nabla d^1_\star$ are finite and non-zero, $\|\nabla g_\star \times \nabla d^1_\star\|$ must approach zero with the same order as their included angle, i.e., $\|\nabla g_\star \times \nabla d^1_\star\| \sim \angle(\nabla d^1_\star, \nabla g_\star) > 0$. Similarly, $\|\nabla g_\star \times \nabla d^2_\star\| \sim \angle(\nabla g_\star, \nabla d^2_\star) > 0$ and $\|\nabla d^2_\star \times \nabla d^1_\star\| \sim \angle(\nabla d^1_\star, \nabla d^2_\star) > 0$. Since $\nabla g_\star$ is in between $\nabla d^1_\star$, $\nabla d^2_\star$, it holds that $\angle(\nabla d^1_\star, \nabla d^2_\star) = \angle(\nabla d^1_\star, \nabla g_\star) + \angle(\nabla g_\star, \nabla d^2_\star)$. Note the two

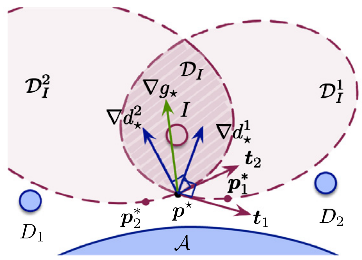

Fig. 7. Relative orientations of ∇g, ∇d^1 and ∇d^2.

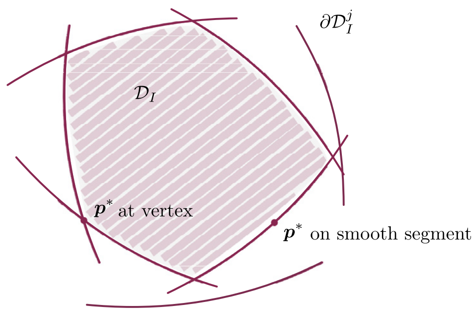

Fig. 8. Dominance region in MDSI game.

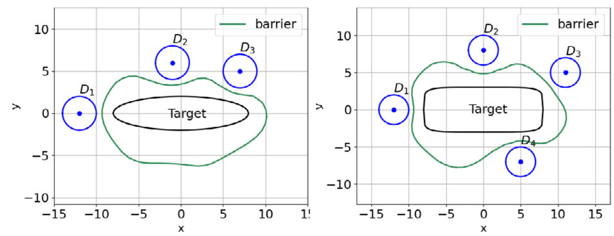

(a) $\phi(x, y) = (x/8)^2 + (y/2)^2 - 1$ (b) $\phi(x, y) = (x/8)^6 + (y/3)^6 - 1$

Fig. 9. Barrier of the MDSI game. $v_D = 1.5$, $v_I = 1$, $r = 2$.

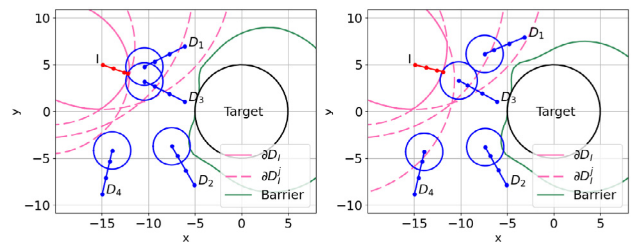

(a) Degenerated as a 2DSI game (b) Degenerated as an SDSI game

Fig. 10. 4DSI game simulations. $\phi(x, y) = \sqrt{x^2 + y^2} - 5$.

defenders are identical, we only label them as D_1, D_2 for the ease of discussion. As $\angle(\nabla d_\star^1, \nabla d_\star^2) \to 0$, there is no reason one of $\angle(\nabla d_\star^1, \nabla g_\star)$, $\angle(\nabla g_\star, \nabla d_\star^2)$ approaches zero at the same order of $\angle(\nabla d_\star^1, \nabla d_\star^2)$ but the other does not. This means limits

$$\lim_{\angle(\nabla d_\star^1, \nabla d_\star^2)\to 0} \frac{\angle(\nabla d_\star^1, \nabla g_\star)}{\angle(\nabla d_\star^1, \nabla d_\star^2)}, \quad \lim_{\angle(\nabla d_\star^1, \nabla d_\star^2)\to 0} \frac{\angle(\nabla g_\star, \nabla d_\star^2)}{\angle(\nabla d_\star^1, \nabla d_\star^2)}$$

are both finite. Consequently, (4.7) is finite even when $\Omega \to 0$.

4.4. Proof for the MDSI game

Since $\mathcal{D}_I = \cap_{i=1,\dots,n}\mathcal{D}_I^j$, $\partial\mathcal{D}_I$ is piece-wise smooth, where each segment belongs to one of $\partial\mathcal{D}_I^1, \dots, \partial\mathcal{D}_I^n$ (Fig. 8). Then $\boldsymbol{p}^*$ can take two kinds of locations, within a smooth segment $\partial\mathcal{D}_I$ or at a vertex. In the former case, the game degenerates into an SDSI game. In the latter case, the game degenerates as a 2DSI game. So the HJI equation is satisfied within each case.

Because the differentiability of V^g is not assured when the game switches cases, we prove V^g to be continuous thus it satisfies the HJI equation in the viscosity sense (Crandall & Lions, 1983). On the one hand, if the MDSI game degenerates as an SDSI game with D_j, there must exist a small enough deviation in player locations such that the relationship $\boldsymbol{p}^* = \boldsymbol{p}_j^*$ is maintained, so the continuity of $\boldsymbol{p}^*$ is inherited from $\boldsymbol{p}_j^*$. On the other hand, if the MDSI game degenerates as a 2DSI game with D_{j_1}, D_{j_2}, then the new degenerated game after the deviation must remain as a game with either or both of D_{j_1}, D_{j_2}. This is because other vertices of $\partial\mathcal{D}_I$ are at finite distances away, hence $\boldsymbol{p}^*$ will not switch to other vertices under small enough deviations. So the continuity of $\boldsymbol{p}^*$ follows from the 2DSI game. For the 2DSI game, we only need to consider switches involving the non-degenerated game. Note the switch happens when $\boldsymbol{p}_1^*, \boldsymbol{p}_2^*, \boldsymbol{p}^\star$ overlap, therefore the continuity of the value function follows from the continuity of $\boldsymbol{p}_1^*$, $\boldsymbol{p}_2^*$, $\boldsymbol{p}^\star$, which has been asserted in the previous sections.

4.5. Simulations

This section shows some simulations of the geometric solution. The (non-dimensional) parameters used are $v_D = 1.5$, $v_I = 1$, $r = 2$. Given defender locations, the location for the invader to win the game is given by $\{[x, y]^T | V(x_1, y_1, \dots, x_n, y_n, x, y) < 0\}$. The boundary of this region is called the barrier. The barrier for different target areas are shown in Fig. 9.

Trajectories of an MDSI game with four defenders are shown in Fig. 10. This game is always degenerated. When the game degenerates as a 2DSI game, the invader is captured at a vertex of $\partial\mathcal{D}_I$. when the game degenerates as an SDSI game, the invader is captured at a smooth segment of $\partial\mathcal{D}_I$.

5. Conclusion and future work

This paper justifies an existing geometric solution of a multiplayer target defense game with non-zero capture ranges and an arbitrary convex target area. The dominance region boundary of this game is a fourth-order curve and the target area takes no specific form, which makes the derivatives of the value function V^g tricky to compute. We resolve this challenge by constructing an implicit function of the intermediate variable $\boldsymbol{p}^*$, re-organizing the HJI equation, and appropriate choice of reference frames. By investigating how the MDSI game degenerates, we simplify the problem as an SDSI or a 2DSI game.

To extend this work, the second-order differentiability requirement on ϕ can be relaxed. The authors' supposition is that continuity is sufficient. One may also consider multiple invaders, but it is more challenging because a task assignment problem is needed to decide the capture order (Fu & Liu, 2021), and the number of players changes when an invader is captured.

Acknowledgment

The research work presented here is sponsored by the Natural Sciences and Engineering Research Council of Canada (NSERC), under its CREATE program, Grant 466088-2015.

Appendix A. Partial derivatives of $\boldsymbol{d}$, $\boldsymbol{k}$

Since d, k are represented with R_D, R_I, α, β, we will start with derivatives of R_D, R_I, α, β. This appendix adopts the SDSI notations in Table 1, but the result can be used for MDSI games by replacing $\boldsymbol{p}_D = [x_D, y_D]^T$ with $\boldsymbol{p}_j = [x_j, y_j]^T$.

A.1. Derivatives of R_D, R_I, α, β

According to the definition of R_D in (2.5c) and α in (3.4),

$$(R_D)_x = \frac{\partial R_D}{\partial x} = \frac{\partial}{\partial x}\sqrt{(x-x_D)^2+(y-y_D)^2} \tag{A.1a}$$
$$= \frac{2(x-x_D)}{2\sqrt{(x-x_D)^2+(y-y_D)^2}} = \cos\alpha. \tag{A.1b}$$

To compute $(R_D)_y$, we can replace $(x-x_D)$ with $(y-y_D)$ in the numerator of (A.1b) and the result yields $(R_D)_y = \sin\alpha$. Further, it can be seen that the only difference between $(R_D)_x$ and $(R_D)_{x_D}$ is x having coefficient $+1$ in $(x-x_D)$ while x_D having -1. Therefore $(R_D)_{x_D} = -(R_D)_x$. Similarly, $(R_D)_{y_D} = -(R_D)_y$. This concludes all the first order partial derivatives of R_D. Since R_I is defined the same way as R_D, derivatives of R_I can be inferred from that of R_D with α replaced by β and x_D, y_D replaced with x_I, y_I. The results are listed in Eq. (A.2).

$$\begin{aligned}
&(R_D)_x = \cos\alpha, && (R_D)_y = \sin\alpha\\
&(R_D)_{x_D} = -\cos\alpha, && (R_D)_{y_D} = -\sin\alpha\\
&(R_I)_x = \cos\beta, && (R_I)_y = \sin\beta\\
&(R_I)_{x_I} = -\cos\beta, && (R_I)_{y_I} = -\sin\beta
\end{aligned} \tag{A.2}$$

To compute partial derivatives of $\cos\alpha$, multiply both sides of the first equation in (3.4a) by R_D and obtain

$$R_D\cos\alpha = x - x_D. \tag{A.3}$$

Taking derivative of (A.3) over x, x_D, y, y_D respectively gives

$$(R_D)_x\cos\alpha + R_D(\cos\alpha)_x = 1 \tag{A.4a}$$
$$(R_D)_{x_D}\cos\alpha + R_D(\cos\alpha)_{x_D} = -1. \tag{A.4b}$$
$$(R_D)_y\cos\alpha + R_D(\cos\alpha)_y = 0 \tag{A.4c}$$
$$(R_D)_{y_D}\cos\alpha + R_D(\cos\alpha)_{y_D} = 0 \tag{A.4d}$$

from which we can solve

$$\begin{aligned}
&(\cos\alpha)_x = \sin^2\alpha/R_D, && (\cos\alpha)_y = -\sin\alpha\cos\alpha/R_D,\\
&(\cos\alpha)_{x_D} = -\sin^2\alpha/R_D, && (\cos\alpha)_{y_D} = \sin\alpha\cos\alpha/R_D.
\end{aligned} \tag{A.5a}$$

Repeating this process for the other equation of (3.4a) gives

$$\begin{aligned}
&(\sin\alpha)_x = -\sin\alpha\cos\alpha/R_D, && (\sin\alpha)_y = \cos^2\alpha/R_D,\\
&(\sin\alpha)_{x_D} = \sin\alpha\cos\alpha/R_D, && (\sin\alpha)_{y_D} = -\cos^2\alpha/R_D.
\end{aligned} \tag{A.5b}$$

Because R_I, β are defined the same way as R_D, α, derivatives regarding β can be inferred from (A.5a) (A.5b) by replacing subscript $_D$ with $_I$, and replacing angle α with β. The result is

$$\begin{aligned}
&(\cos\beta)_x = \sin^2\beta/R_I, && (\cos\beta)_y = -\sin\beta\cos\beta/R_I,\\
&(\cos\beta)_{x_I} = -\sin^2\beta/R_I, && (\cos\beta)_{y_I} = \sin\beta\cos\beta/R_I,\\
&(\sin\beta)_x = -\sin\beta\cos\beta/R_I, && (\sin\beta)_y = \cos^2\beta/R_I,\\
&(\sin\beta)_{x_I} = \sin\beta\cos\beta/R_I, && (\sin\beta)_{y_I} = -\cos^2\beta/R_I.
\end{aligned} \tag{A.5c}$$

A.2. Derivatives of d

Recall $d = R_D - aR_I - r$. Based on the derivatives of R_D, R_I, first order derivatives of d can be computed directly:

$$\begin{aligned}
&d_x = \cos\alpha - a\cos\beta, && d_y = \sin\alpha - a\sin\beta,\\
&d_{x_D} = -\cos\alpha, && d_{y_D} = -\sin\alpha,\\
&d_{x_I} = a\cos\beta, && d_{y_I} = a\sin\beta.
\end{aligned} \tag{A.6}$$

Second order derivatives of d can be obtained by differentiating (A.6) and using (A.5). Here we only list those will be used to compute the derivatives of k:

$$\begin{aligned}
&d_{xx} = \sin^2\alpha/R_D - a\sin^2\beta/R_I,\\
&d_{xy} = -\sin\alpha\cos\alpha/R_D + a\sin\beta\cos\beta/R_I,\\
&d_{yy} = \cos^2\alpha/R_D - a\cos^2\beta/R_I,\\
&d_{xx_D} = -\sin^2\alpha/R_D, \qquad d_{xy_D} = \sin\alpha\cos\alpha/R_D,\\
&d_{xx_I} = a\sin^2\beta/R_I, \qquad d_{xy_I} = -a\sin\beta\cos\beta/R_I,\\
&d_{yx_D} = \sin\alpha\cos\alpha/R_D, \qquad d_{yy_D} = -\cos^2\alpha/R_D,\\
&d_{yx_I} = -a\sin\beta\cos\beta/R_I, \qquad d_{yy_I} = a\cos^2\beta/R_I.
\end{aligned} \tag{A.7}$$

A.3. Derivatives of k

Recall $k = -d_x/d_y$, so k_{x_D} can be computed as

$$k_{x_D} = -\frac{d_{xx_D}}{d_y} + d_x\frac{d_{yx_D}}{d_y^2} = \frac{d_x d_{yx_D} - d_y d_{xx_D}}{d_y^2}. \tag{A.8}$$

k_x, k_y, k_{y_D}, k_{x_I}, k_{y_I} can be obtained by replacing subscript x_D with x, y, y_D, x_I, y_I. Substituting second order derivatives of d from (A.7) and using (3.5), we have

$$\begin{aligned}
&k_x = \rho_D\sin\alpha + a\rho_I\sin\beta, && k_y = -\rho_D\cos\alpha - a\rho_I\cos\beta,\\
&k_{x_D} = -\rho_D\sin\alpha, && k_{y_D} = \rho_D\cos\alpha,\\
&k_{x_I} = -a\rho_I\sin\beta, && k_{x_I} = a\rho_I\cos\beta.
\end{aligned} \tag{A.9}$$

Appendix B. Details in computing derivatives of x^*, y^*

B.1. Derivatives of x^*, y^* w.r.t. x_D

As stated in Section 3.3.2, taking derivatives of (3.11) over x_D gives (3.13). Re-organizing it using (3.14) gives

$$\begin{aligned}
G_{x^*}x^*_{x_D} + G_{y^*}y^*_{x_D} + \phi_{y^*}k_{x^*_D} = 0,\\
d_{x^*}x^*_{x_D} + d_{y^*}y^*_{x_D} + d_{x^*_D} = 0,
\end{aligned} \tag{B.1}$$

where G_{x^*}, G_{y^*} are derivatives of ϕ, d, k grouped together:

$$G_{x^*} = K_*^T\nabla\phi_{x^*} + k_{x^*}\phi_{y^*}, \quad G_{y^*} = K_*^T\nabla\phi_{y^*} + k_{y^*}\phi_{y^*}.$$

Then, it can be solved from (B.1) that

$$x^*_{x_D} = \left(d_{x^*_D}G_{y^*} - k_{x^*_D}d_{y^*}\phi^*_y\right)/\Delta, \tag{B.2a}$$
$$y^*_{x_D} = -\left(d_{x^*_D}G_{x^*} - k_{x^*_D}d_{x^*}\phi_{y^*}\right)/\Delta, \tag{B.2b}$$
$$\Delta = d_{y^*}G_{x^*} - d_{x^*}G_{y^*}. \tag{B.2c}$$

In (B.2a), putting Δ on the left-hand-side, expand G_{y^*}, and substituting the expressions of d_{x^*}, d_{y^*}, $d_{x^*_D}$, we have

$$\begin{aligned}
x^*_{x_D}\Delta &= -\cos\alpha_*\left[K_*^T\nabla\phi_{y^*} - \left(\rho_D^*\cos\alpha_* + a\rho_I^*\cos\beta_*\right)\phi_{y^*}\right]\\
&\quad + \rho_D^*\sin\alpha_*\left(\sin\alpha_* - a\sin\beta_*\right)\phi_{y^*}\\
&= -K_*^T\nabla\phi_{y^*}\cos\alpha_* + \rho_D^*\phi_{y^*}\\
&\quad + a\rho_I^*\cos\alpha_*\cos\beta_*\phi_{y^*} - a\rho_D^*\sin\alpha_*\sin\beta_*\phi_{y^*}\\
&= -K_*^T\nabla\phi_{y^*}\cos\alpha_* + \left(\rho_D^* - a\tilde{\boldsymbol{e}}_{\alpha^*}^T R_- \tilde{\boldsymbol{e}}_{\beta^*}\right)\phi_{y^*}.
\end{aligned}$$

This gives (3.15a). Similarly,

$$\begin{aligned}
-y^*_{x_D}\Delta &= -\cos\alpha_*\left[K_*^T\nabla\phi_{x^*} + \left(\rho_D^*\sin\alpha_* + a\rho_I^*\sin\beta_*\right)\phi_{y^*}\right]\\
&\quad + \rho_D^*\sin\alpha_*(\cos\alpha_* - a\cos\beta_*)\phi_{y^*}\\
&= -K_*^T\nabla\phi_{x^*}\cos\alpha_* - a\rho_I^*\sin\beta_*\cos\alpha_*\phi_{y^*}\\
&\quad - a\rho_D^*\sin\alpha_*\cos\beta_*\phi_{y^*}\\
&= -K_*^T\nabla\phi_{x^*}\cos\alpha_* - \left(a\tilde{\boldsymbol{e}}_{\alpha^*}R_+\boldsymbol{e}_{\beta^*}\right)\phi_{y^*}.
\end{aligned}$$

This gives (3.15b). Other derivatives in (3.15) can be obtained in the same manner.

B.2. Simplify $\varDelta$

Recalling Eq. (3.7) states that $\phi_{x^*}/\phi_{y^*} = d_{x^*}/d_{y^*}$. In addition, $k_* = -d_{x^*}/d_{y^*}$ by (3.3). Then $\varDelta$ can be simplified as

$$\varDelta = d_{y^*}(G_{x^*} - \frac{d_{x^*}}{d_{y^*}} G_{y^*}) = d_{y^*}(G_{x^*} + k_* G_{y^*})$$

Expanding G_{x^*}, G_{y^*} and K_*, $\nabla\phi_{x^*}$, $\nabla\phi_{y^*}$ therein, we have

$$\begin{aligned}\varDelta =& d_{y^*}\left(K_*^T \nabla\phi_{x^*} + k_{x^*}\phi_{y^*} + k_*\left(K_*^T\nabla\phi_{y^*} + k_{y^*}\phi_{y^*}\right)\right)\\ =& d_{y^*}\left[\phi_{xx^*} + k_*\phi_{xy^*} + (k_{x^*} + k_* k_{y^*})\phi_{y^*} + k_*(\phi_{yx^*} + k_*\phi_{yy^*})\right]\\ =& d_{y^*}\left(\frac{d\phi_{x^*}}{dx} + \frac{dk_*}{dx}\phi_{y^*} + k_*\frac{d\phi_{y^*}}{dx}\right)\Bigg|_{\partial\mathcal{D}_I}\\ =& d_{y^*}\left.\frac{d\left(\phi_{x^*} + k_*\phi_{y^*}\right)}{dx}\right|_{\partial\mathcal{D}_I} = d_{y^*}\frac{d}{dx}\left.\left(\frac{d\phi_*}{dx}\right)\right|_{\partial\mathcal{D}_I} = d_{y^*}\left.\frac{d^2\phi_*}{dx^2}\right|_{\partial\mathcal{D}_I}\end{aligned} \tag{B.4}$$

Note in the computation above, subscript $_{\partial\mathcal{D}_I}$ means the derivative is taken along $\partial\mathcal{D}_I$, or equivalently, under constraint $d(x, y, x_D, y_D, x_I, y_I) = 0$. Here x_D, y_D, x_I, y_I are treated as parameters.

Starting from the first line of (B.4), $\varDelta$ can be manipulated in another direction:

$$\begin{aligned}\varDelta =& d_{y^*}\left(K_*^T \nabla\phi_{x^*} + k_{x^*}\phi_{y^*} + k_*\left(K_*^T\nabla\phi_{y^*} + k_{y^*}\phi_{y^*}\right)\right)\\ =& d_{y^*}\left(K_*^T\left[\nabla\phi_{x^*}, \nabla\phi_{x^*}\right]\begin{bmatrix}1\\ k_*\end{bmatrix} + (k_{x^*} + k_* k_{y^*})\phi_{y^*}\right)\\ =& d_{y^*}\left(K_*^T H_{\phi_*} K_* + (k_* k_{y^*} + k_{x^*})\phi_{y^*}\right)\end{aligned} \tag{B.5}$$

This proves Eq. (3.20).

B.3. Inner and cross products of $\boldsymbol{\gamma}_D^1$ with $\boldsymbol{e}_{\alpha^*}$

Inner and cross products of $\boldsymbol{\gamma}_D^1$, $\boldsymbol{\gamma}_D^2$ with $\boldsymbol{e}_{\alpha^*}$ are straightforward to compute by definition. For $\boldsymbol{\gamma}_D^1$, we have

$$\boldsymbol{e}_{\alpha^*}\cdot\boldsymbol{\gamma}_D^1\varDelta = \left(\rho_D^* - a\tilde{\boldsymbol{e}}_{\alpha^*}^T R_- \tilde{\boldsymbol{e}}_{\beta^*}\right)\cos\alpha_* + \left(a\boldsymbol{e}_{\alpha^*}^T R_+\tilde{\boldsymbol{e}}_{\beta^*}\right)\sin\alpha_*.$$

Expand R_-, R_+, $\boldsymbol{e}_{\alpha^*}$, $\boldsymbol{e}_{\beta^*}$, the equation above becomes

$$\begin{aligned}&\boldsymbol{e}_{\alpha^*}\cdot\boldsymbol{\gamma}_D^1\varDelta\\ =& \rho_D^*\cos\alpha_* - a(\rho_D^*\sin\alpha_*\sin\beta_* - \rho_I^*\cos\alpha_*\cos\beta_*)\cos\alpha_* +\\ & a(\rho_D^*\cos\alpha_*\sin\beta_* + \rho_I^*\sin\alpha_*\cos\beta_*)\sin\alpha_*\\ =& \rho_D^*\cos\alpha_* + a\rho_I^*\cos\beta_* = -k_{y^*}.\end{aligned} \tag{B.6}$$

Similarly,

$$\begin{aligned}&\boldsymbol{e}_{\alpha^*}\times\boldsymbol{\gamma}_D^1\varDelta\\ =& -\left(\rho_D^* - a\tilde{\boldsymbol{e}}_{\alpha^*}^T R_-\tilde{\boldsymbol{e}}_{\beta^*}\right)\sin\alpha_* + \left(a\boldsymbol{e}_{\alpha^*}^T R_+\tilde{\boldsymbol{e}}_{\beta^*}\right)\cos\alpha_*\\ =& -\rho_D^*\sin\alpha_* + a(\rho_D^*\sin\alpha_*\sin\beta_* - \rho_I^*\cos\alpha_*\cos\beta_*)\sin\alpha_* +\\ & a(\rho_D^*\cos\alpha_*\sin\beta_* + \rho_I^*\sin\alpha_*\cos\beta_*)\cos\alpha_*\\ =& -\rho_D^*\sin\alpha_* + a\rho_D^*\sin\beta_* = -\rho_D^* d_{y^*}.\end{aligned} \tag{B.7}$$

Using (B.6) (B.7) in (3.18) gives the first equation of (3.19).

B.4. Represent $\partial_{\boldsymbol{p}_I}V$ in $\mathcal{F}_{\beta^*}^*$

Let

$$\boldsymbol{\gamma}_I^1 = \begin{bmatrix} a\rho_I^* + \boldsymbol{e}_{\alpha^*}^T R_-\boldsymbol{e}_{\beta^*}\\ \boldsymbol{e}_{\alpha^*}^T R_+\tilde{\boldsymbol{e}}_{\beta^*}\end{bmatrix}/\varDelta, \quad \boldsymbol{\gamma}_I^2 = \begin{bmatrix}\tilde{\boldsymbol{e}}_{\alpha^*}^T R_+\boldsymbol{e}_{\beta^*}\\ a\rho_I^* + \tilde{\boldsymbol{e}}_{\alpha^*}^T R_-\tilde{\boldsymbol{e}}_{\beta^*}\end{bmatrix}/\varDelta,$$

$\partial_{\boldsymbol{p}_I}V$ can be represented as

$$\partial_{\boldsymbol{p}_I}V^g = -a\phi_{y^*}K_*^T H_{\phi_*}K_*\boldsymbol{e}_{\beta^*}/\varDelta - a\phi_{y^*}^2(-k_*\boldsymbol{\gamma}_I^1 + \boldsymbol{\gamma}_I^2). \tag{B.8}$$

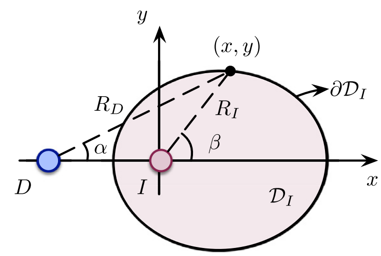

Fig. C.11. Dominance region of the invader under a frame where the x-axis is along $\vec{DI}$.

Following a similar process as Appendix B.3, we can reach

$$\left[\boldsymbol{\gamma}_I^1\right]_{\mathcal{F}_{\beta^*}^*} = -\begin{bmatrix}k_{y^*}\\ d_{y^*}\rho_I^*\end{bmatrix}/\varDelta, \quad \left[\boldsymbol{\gamma}_I^2\right]_{\mathcal{F}_{\beta^*}^*} = \begin{bmatrix}k_{x^*}\\ d_{x^*}\rho_I^*\end{bmatrix}/\varDelta. \tag{B.9}$$

Appendix C. Proof of Lemma 2.1

Since the intersection of convex sets is still convex, we only need to prove the lemma for the SDSI game. Here we use the SDSI game notation from Table 1. Because the convexity of $\mathcal{D}_I$ is independent of the reference frame, we place the x-axis along vector $\vec{DI}$, as shown in Fig. C.11. Since $\partial\mathcal{D}_I$ is described by $d(x, y, x_D, y_D, x_I,$
$y_I) = 0$, an implicit function of $y(x)$, it is sufficient to prove $y(x)$ being concave ($d^2y/dx^2 < 0$) for $y > 0$, and convex ($d^2y/dx^2 > 0$) for $y < 0$. Recall the slope of $\partial\mathcal{D}_I$ is given by $k = -d_x/d_y$, hence d^2y/dx^2 can be computed as

$$\frac{d^2y}{dx^2} = \frac{dk}{dx} = k_x + kk_y = k_x - \frac{d_x}{d_y}k_y = \frac{d_y k_x - d_x k_y}{d_y}.$$

Putting d_y on the left-hand-side, substituting d_x, d_y from (A.6) and k_x, k_y from (A.9), the equation above becomes

$$\begin{aligned} d_y\frac{d^2y}{dx^2} =& (\sin\alpha - a\sin\beta)(\rho_D\sin\alpha + a\rho_I\sin\beta)\\ & + (\cos\alpha - a\cos\beta)(\rho_D\cos\alpha + a\rho_I\cos\beta)\\ =& \rho_D - a^2\rho_I - a\rho_D\cos(\alpha-\beta) + a\rho_I\cos(\alpha-\beta)\\ =& -\rho_D\left(a\cos(\alpha-\beta) - 1\right) + a\rho_I(\cos(\alpha-\beta) - a)\\ =& -\frac{(a\cos(\alpha-\beta)-1)^2}{(d_y)^2 R_D} + \frac{a\left(\cos(\alpha-\beta)-a\right)^2}{(d_y)^2 R_I}\end{aligned}$$

According to the definition of R_D, R_I in (2.5c) and a in (2.3), and the fact that $a \geq 1$, it must hold that $R_I/R_D < 1$. Multiplying both sides of the equation above by $(d_y)^2 R_I$, we have

$$\begin{aligned}(d_y)^3 R_I\frac{d^2y}{dx^2} =& -\left(a\cos(\alpha-\beta)-1\right)^2\frac{R_I}{R_D} + a\left(\cos(\alpha-\beta)-a\right)^2\\ >& -\left(a\cos(\alpha-\beta)-1\right)^2 + \left(\cos(\alpha-\beta)-a\right)^2\\ =& \left(a^2-1\right)\left(1-\cos^2(\alpha-\beta)\right) \geq 0\end{aligned}$$

This means the sign of d^2y/dx^2 is the same as d_y. According to (A.6), $d_y = \sin\alpha - a\sin\beta$. In the chosen reference frame, $y_D = y_I = 0$. Using this in the definition of α, β, it can be seen that $|\sin\alpha| < |\sin\beta|$. As a result, we have $\sin\alpha - a\sin\beta < 0$ for $y > 0$, and $\sin\alpha - a\sin\beta > 0$ for $y < 0$. This implies $d^2y/dx^2 < 0$ when $y > 0$, and $d^2y/dx^2 > 0$ when $y < 0$.

References

Breakwell, J., & Hagedorn, P. (1979). Point capture of two evaders in succession. *Journal of Optimization Theory and Applications*, *27*(1), 89–97.

Carr, R. W., Cobb, R. G., Pachter, M., & Pierce, S. (2018). Solution of a Pursuit–Evasion game using a near-optimal strategy. *Journal of Guidance, Control, and Dynamics*, *41*(4), 841–850.
Crandall, M. G., & Lions, P.-L. (1983). Viscosity solutions of Hamilton-Jacobi equations. *Transactions of the American Mathematical Society*, *277*(1), 1–42.
Dixon, W. (2014). Optimal adaptive control and differential games by reinforcement learning principles.
Dorothy, M., Maity, D., Shishika, D., & Von Moll, A. (2021). One apollonius circle is enough for many pursuit-evasion games. arXiv preprint arXiv:2111.09205.
Falcone, M. (2006). Numerical methods for differential games based on partial differential equations. *International Game Theory Review*, *8*(02), 231–272.
Fisac, J. F., Chen, M., Tomlin, C. J., & Sastry, S. S. (2015). Reach-avoid problems with time-varying dynamics, targets and constraints. In *Proceedings of the 18th international conference on hybrid systems: Computation and control* (pp. 11–20).
Fu, H., & Liu, H. H.-T. (2020). Guarding a territory against an intelligent intruder: Strategy design and experimental verification. *IEEE/ASME Transactions on Mechatronics*, *25*(4), 1765–1772.
Fu, H., & Liu, H. H. (2021). On the strategies of defending a target against multiple intruders. In *AIAA scitech 2021 forum* (p. 1861). http://dx.doi.org/10.2514/6.2021-1861.
Fuchs, Z. E., Khargonekar, P. P., & Evers, J. (2010). Cooperative defense within a single-pursuer, two-evader pursuit evasion differential game. In *49th IEEE conference on decision and control (CDC)* (pp. 3091–3097). IEEE.
Garcia, E., & Bopardikar, S. D. (2021). Cooperative containment of a high-speed evader. In *2021 American control conference (ACC)* (pp. 4698–4703). IEEE.
Garcia, E., Casbeer, D. W., & Pachter, M. (2020). Optimal strategies for a class of multi-player reach-avoid differential games in 3d space. *IEEE Robotics and Automation Letters*, *5*(3), 4257–4264.
Garcia, E., Casbeer, D. W., Tran, D., & Pachter, M. (2021). A differential game approach for beyond visual range tactics. In *2021 American control conference (ACC)* (pp. 3210–3215). IEEE.
Garcia, E., Von Moll, A., Casbeer, D. W., & Pachter, M. (2019). Strategies for defending a coastline against multiple attackers. In *2019 IEEE 58th conference on decision and control (CDC)* (pp. 7319–7324). IEEE.
Hagedorn, P., & Breakwell, J. (1976). A differential game with two pursuers and one evader. *Journal of Optimization Theory and Applications*, *18*(1), 15–29.
Isaacs, R. (1999). *Differential games: a mathematical theory with applications to warfare and pursuit, control and optimization*. Courier Corporation.
Lee, Y., & Bakolas, E. (2021). Optimal strategies for guarding a compact and Convex Target Area: A differential game approach. arXiv preprint arXiv:2104.00717.
Lee, E. S., Shishika, D., & Kumar, V. (2020). Perimeter-defense game between aerial defender and ground intruder. In *2020 59th IEEE conference on decision and control (CDC)* (pp. 1530–1536). IEEE.
Lowe, R., Wu, Y. I., Tamar, A., Harb, J., Pieter Abbeel, O., & Mordatch, I. (2017). Multi-agent actor-critic for mixed cooperative-competitive environments. *Advances in Neural Information Processing Systems*, *30*.
Margellos, K., & Lygeros, J. (2011). Hamilton–Jacobi formulation for reach–avoid differential games. *IEEE Transactions on Automatic Control*, *56*(8), 1849–1861.
Marzoughi, A., & Savkin, A. V. (2021). Autonomous navigation of a team of unmanned surface vehicles for intercepting intruders on a region boundary. *Sensors*, *21*(1), 297.
Merz, A. W. (1971). *The homicidal chauffeur–a differential game*. Stanford University.
Merz, A. (1972). The game of two identical cars. *Journal of Optimization Theory and Applications*, *9*(5), 324–343.
Michel, A. H., & Holland, A. (2018). *Counter-drone systems*. Center for the Study of the Drone At Bard College.
Mitchell, I. M. (2007). *A toolbox of level set methods*: *UBC Department of Computer Science Technical Report TR-2007-11*.
Mitchell, I. M., Bayen, A. M., & Tomlin, C. J. (2005). A time-dependent Hamilton-Jacobi formulation of reachable sets for continuous dynamic games. *IEEE Transactions on Automatic Control*, *50*(7), 947–957.
Pachter, M., Garcia, E., & Casbeer, D. W. (2017). Differential game of guarding a target. *Journal of Guidance, Control, and Dynamics*, *40*(11), 2991–2998.
Pachter, M., Moll, A. V., Garcia, E., Casbeer, D., & Milutinović, D. (2020). Cooperative pursuit by multiple pursuers of a single evader. *Journal of Aerospace Information Systems*, *17*(8), 371–389.
Ramana, M. V., & Kothari, M. (2017). Pursuit-evasion games of high speed evader. *Journal of Intelligent and Robotic Systems*, *85*(2), 293–306.
Rubies-Royo, V., & Tomlin, C. (2016). Recursive regression with neural networks: Approximating the HJI PDE solution. arXiv preprint arXiv:1611.02739.
Sathyamoorthy, D. (2015). A review of security threats of unmanned aerial vehicles and mitigation steps. *Journal of Defence & Security Technologies*, *6*(1), 81–97.
Scott, W., & Leonard, N. E. (2014). Dynamics of pursuit and evasion in a heterogeneous herd. In *53rd IEEE conference on decision and control* (pp. 2920–2925). IEEE.
Scott, W. L., & Leonard, N. E. (2018). Optimal evasive strategies for multiple interacting agents with motion constraints. *Automatica*, *94*, 26–34.
Shishika, D., & Kumar, V. (2018). Local-game decomposition for multiplayer perimeter-defense problem. In *2018 IEEE conference on decision and control (CDC)* (pp. 2093–2100). IEEE.
Shishika, D., & Kumar, V. (2019). Perimeter-defense game on arbitrary convex shapes. arXiv preprint arXiv:1909.03989.
Shishika, D., & Kumar, V. (2020). A review of multi agent perimeter defense games. In *International conference on decision and game theory for security* (pp. 472–485). Springer.
Shishika, D., Paulos, J., & Kumar, V. (2020). Cooperative team strategies for multi-player perimeter-defense games. *IEEE Robotics and Automation Letters*, *5*(2), 2738–2745.
Szőts, J., & Harmati, I. (2019). A simple and effective strategy of a superior evader in a pursuit-evasion game. In *2019 18th European control conference (ECC)* (pp. 3544–3549). IEEE.
Szőts, J., Savkin, A. V., & Harmati, I. (2021). Revisiting a three-player pursuit-evasion game. *Journal of Optimization Theory and Applications*, *190*(2), 581–601.
Vamvoudakis, K. G., & Lewis, F. L. (2011). Multi-player non-zero-sum games: Online adaptive learning solution of coupled Hamilton–Jacobi equations. *Automatica*, *47*(8), 1556–1569.
Von Moll, A., Casbeer, D., Garcia, E., Milutinović, D., & Pachter, M. (2019). The multi-pursuer single-evader game. *Journal of Intelligent and Robotic Systems*, *96*(2), 193–207.
Von Moll, A., Pachter, M., Shishika, D., & Fuchs, Z. (2020). Guarding a circular target by patrolling its perimeter. In *2020 59th IEEE conference on decision and control (CDC)* (pp. 1658–1665). IEEE.
Wang, H., Yue, Q., & Liu, J. (2015). Research on pursuit-evasion games with multiple heterogeneous pursuers and a high speed evader. In *The 27th Chinese control and decision conference (2015 CCDC)* (pp. 4366–4370). IEEE.
Wei, X., & Yang, J. (2018). Optimal strategies for multiple unmanned aerial vehicles in a pursuit/evasion differential game. *Journal of Guidance, Control, and Dynamics*, *41*(8), 1799–1806.
Weintraub, I. E., Von Moll, A., Garcia, E., Casbeer, D. W., & Pachter, M. (2022). Surveillance of a faster fixed-course target. arXiv preprint arXiv:2209.11289.
Yan, R., Shi, Z., & Zhong, Y. (2018). Reach-avoid games with two defenders and one attacker: An analytical approach. *IEEE Transactions on Cybernetics*, *49*(3), 1035–1046.
Yan, R., Shi, Z., & Zhong, Y. (2019). Task assignment for multiplayer reach–avoid games in convex domains via analytical barriers. *IEEE Transactions on Robotics*, *36*(1), 107–124.
Yan, R., Shi, Z., & Zhong, Y. (2021). Optimal strategies for the lifeline differential game with limited lifetime. *International Journal of Control*, *94*(8), 2238–2251.
Zha, W., Chen, J., Peng, Z., & Gu, D. (2016). Construction of barrier in a fishing game with point capture. *IEEE Transactions on Cybernetics*, *47*(6), 1409–1422.

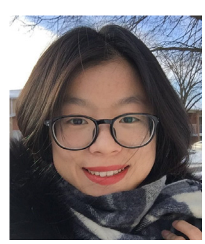

Han Fu is a Ph.D. candidate at the University of Toronto Institute for Aerospace Studies. She received her Bachelor's degree from Shanghai Jiao Tong University in 2015 and started her study at University of Toronto in 2017. Her research interests include differential games and multi-agent systems.

Hugh H.-T. Liu is a Professor of the University of Toronto Institute for Aerospace Studies. He received his Bachelor's degree from Shanghai Jiao Tong University in 1991, Master's degree from Beijing University of Aeronautics and Astronautics in 1994, and Ph.D. from the University of Toronto in 1998. His research interests include autonomous unmanned systems, cooperative and formation control, fault tolerant control, active control on advanced aircraft systems, as well as integrated modeling and simulations. Dr. Liu has served many years as a member of the AIAA Guidance, Navigation, and Control Technical Committee. He currently serves as the Associate Editor of AIAA Journal of Guidance, Control and Dynamics. He is also an Associate Editor of the Canadian Aeronautics and Space Journal, an Associate Fellow of AIAA, a Fellow of Canadian Society of Mechanical Engineers, and a registered Professional Engineer in Ontario, Canada. He was elected to the Canadian Academy of Engineering in 2022.